

The optically–dark side of galaxy formation

Bruno Guiderdoni¹, François R. Bouchet¹, Jean–Loup Puget²,

Guilaine Lagache² & Eric Hivon³

¹ *Institut d’Astrophysique de Paris, CNRS, 98bis Boulevard Arago, F–75014 Paris*

² *Institut d’Astrophysique Spatiale, Bât. 121, Université Paris XI, F–91405 Orsay Cedex*

³ *Theoretical Astrophysics Center, Juliane Maries Vej 30, DK–2100 Copenhagen*

Deep optical surveys [1, 2] probe the rest–frame ultraviolet luminosities of high–redshift galaxies, which can be converted into star formation rates under plausible assumptions on young stellar populations. The current analysis of these data suggests that the global star formation rate of the universe peaked at a redshift of 1 and declined since then [3, 4]. This has led to claims that the bulk of star formation in the universe has been seen. However, the conversion of UV luminosities into star formation rates must take into account a correction for the luminosity fraction absorbed by the dust which is generically associated to young stars. Since this correction is rather uncertain for high–redshift galaxies, the star formation rates currently deduced from optical surveys alone might be substantially underestimated. To circumvent this problem, the simplest is to observe the dust thermal emission at infrared (and submillimetre) wavelengths and compute the overall luminosity budget of galaxies. For high–redshift galaxies,

the only direct observational constraint is set by the recent detection of the Cosmic Infrared Background (CIRB) built up from the accumulated IR light of faint galaxies along the line of sight [5]. Here we propose a more accurate determination of this long-sought background which solves the main possible weakness of the earlier determination. Then we estimate the population of high-redshift, dust-enshrouded starburst galaxies needed to produce this background. We argue that most of the star formation at high redshift may be hidden by dust, and we define the necessary characteristics of a feasible survey at a wavelength of $175 \mu\text{m}$, which could detect this population.

While only one third of the bolometric luminosity of local galaxies is radiated in the IR [6], there is a growing evidence that this fraction is actually increasing with redshift. The deepest counts available from the Infrared Astronomical Satellite (IRAS) at $60 \mu\text{m}$ [7], which correspond to an average redshift z of only 0.2 [8], already suggest some evolution of the IR emission in the universe. A recent deep survey with the Infrared Space Observatory (ISO) at $15 \mu\text{m}$ has discovered a few objects at $z \sim 0.5$ to 1 with star formation rates much higher than deduced from the optical [9]. However, the strongest constraint on the high-redshift IR emission is given by the CIRB found in data acquired by the FIRAS instrument on-board the COBE satellite in the $200 \mu\text{m} - 2 \text{mm}$ wavelength range [5]. Several steps are necessary in order to remove the foreground Galactic components and extract the isotropic residual identified as the CIRB. While, at the wavelengths probed by FIRAS, the interplanetary emission is small and easily removed [10], the emission from interstellar dust mixed with the different gas phases of the interstellar medium is the dominant component. The spectra which correlate with the 21 cm interstellar emission of neutral hydrogen (HI) [11] along lines-of-sight with HI column densities $N_{HI} \leq 4.5 \times 10^{20} \text{ atoms cm}^{-2}$ are described by a modified black-body $\nu^2 B_\nu(T)$ with $T = 17.5 \text{ K}$ [12]. Part of the long-wavelength excess over this simple model increases with HI column density and can be linked to dust emission associated with ionized and molecular hydrogen. The other part is an isotropic residual which

has been interpreted as the CIRB. The determination of the isotropy required to use a large fraction of the sky. This thus involved correcting for substantial foreground components. Any inaccuracy in this correction might have contributed a spurious signal. In order to address this problem, the original method of Puget *et al.* [5] was applied again, but only in the cleanest regions with very low HI column densities ($N_{HI} \leq 1 \times 10^{20}$ atoms cm^{-2} instead of $N_{HI} \leq 4.5 \times 10^{20}$ atoms cm^{-2}). In that case, the residual component totally dominates the emission (inset in fig.1). This demonstrates that it cannot be due to artifacts in the removal of interstellar emission. Fig.1 also shows that the CIRB intensity per frequency decade $\nu I_\nu = 7 \cdot 10^{-9}$ W m^{-2} sr^{-1} near 300 μm is a factor of 5 higher than the no-evolution prediction obtained by a simple extrapolation of the IR luminosities of local galaxies. Its level is comparable to that of the ‘‘Cosmic Optical Background’’ estimated by summing up faint galaxy counts down to the deepest limit so far available which is given by the Hubble Deep Field [2].

In order to break the background into the contributing sources, we need to model the IR/submm emission of galaxies. Galaxy formation and evolution can be briefly sketched as follows: Small fluctuations in the high- z universe grow by gravitational instability until they form dense clumps where the baryonic gas is collisionally heated. Where the density and temperature are appropriate, gas cools by emitting radiation, and the baryons pile up in cold cores whose final radii are set by angular-momentum conservation. Simultaneously, larger clumps form and encompass/accrete the previous generation of small clumps. Stars form in the cores and enrich the primordial gas via supernova ejecta. Part of the starlight is absorbed by various dust components which re-radiate at longer wavelengths according to characteristic IR spectra. The so-called ‘‘semi-analytic modelling’’ of these series of physical processes has been rather successful in reproducing the overall properties of galaxies in the optical range [14, 15]. We have elaborated an extension of this method to the IR/submm range. Details of the modelling, and complementary predictions will be given elsewhere [16, 17].

Specifically, we assume a standard Cold Dark Matter cosmological model [18] with a Hubble constant $H_0 = 50 \text{ km s}^{-1} \text{ Mpc}^{-1}$, a density parameter $\Omega_0 = 1$, a cosmological constant $\Lambda = 0$, a baryon fraction $\Omega_b = 0.05$, and a normalisation $\sigma_8 = 0.67$ for the power spectrum of linear fluctuations. The sensitivity of the semi-analytic modelling to cosmological parameters is known to be weak [19]. In our reference scenario A, we consider a mix of two broad types of populations, one with low star formation rates (which reproduce the observational distribution of gas consumption time scales in disk galaxies [20]), the other proceeding in bursts with ten times larger star formation rates. We assume that bursts are triggered by interaction and merging of sub-galactic clumps [21], and increase with z according to the fraction of pairs [22, 23, 24]. This population of “mild starbursts” and “luminous UV/IR galaxies” (similar to “LIRGs” [25]) dominate the optical background (fig.1). The IR luminosity-to-mass ratio is $L_{IR}/M = 6L_{bol\odot}/M_\odot$ for a typical starburst with $t_\star = 0.33$ Gyr. The range of derived IR-to-blue luminosity ratios is characteristic of blue-band selected samples [26] like the Canada-France Redshift Survey (selected in the observer-frame I_{AB} band, roughly corresponding to the B band at $z \sim 1$), or the high- z galaxies of the Hubble Deep Field. Fig.1 also displays the predicted IR background, which is clearly barely compatible with the observed CIRB whose mean amplitude is twice higher.

In order to assess how much star formation might be *completely* hidden by dust shrouds, we consider an additional population, similar to “ultra-luminous IR galaxies” (“ULIRGs”) [25]. We maximize their IR luminosities by assuming that all the energy available from stellar nucleosynthesis is radiated by massive stars and heats up the dust. As a consequence of a stellar initial mass function with short-lived, massive stars, the post-starburst phase is “dark” and would be detectable only by its nucleosynthesis products. The luminosity-to-mass ratio now is $L_{IR}/M = 130L_{bol\odot}/M_\odot$ for a typical starburst with $t_\star = 0.33$ Gyr. Our scenarios B and C respectively mimic continuous bulge formation as the end-product of interaction and merging, and a strong episode of bulge formation at $z_{for} > 3.5$. Both are consistent with the observed CIRB. The high-redshift, dust-enshrouded, star formation in

scenario C results in the high level of the predicted background at wavelengths $\lambda > 400 \mu\text{m}$.

While none of the currently available optical data reflects the large differences between these scenarios, originating in the different fractions of heavily-extinguished objects, the predicted IR/submm counts are more interesting, as shown in fig.2. The comparison of IRAS data with the no-evolution curve at $60 \mu\text{m}$ suggests some evolution. However, it appears that the $60 \mu\text{m}$ band does not strongly discriminate between the various scenarios of evolution. In contrast, the upward deviation at $200 \mu\text{m}$ is due to the contribution of the redshifted $100 \mu\text{m}$ maximum of the IR energy distribution. This redshifting of steep spectra counter-balances distance dimming and can make high- z objects *easier* to detect than low- z ones. Submm observations are thus quite sensitive to the high- z history. The model also predicts that, at $200 \mu\text{m}$, 10–100 mJy sources (contributing to 15 % of the background) are mostly located at $z \sim 0.5 - 2.5$, while at $60 \mu\text{m}$, and at the typical sensitivity level of IRAS surveys, the sources are indeed located mostly at very low z .

The detection of these sources would be a strong test for assessing the level of the “optically-dark” side of galaxy formation. The C160 filter of the ISOPHOT instrument on-board ISO has an effective wavelength $\lambda_{eff} \simeq 175 \mu\text{m}$ for typical spectra of distant galaxies, and a 10 mJy *rms* noise fluctuation per 1.5 arcmin pixel is reachable after integration times larger than ~ 256 s per pixel. Thus a deep survey with this instrument appears to be feasible and is indeed scheduled. However, one might be concerned that small-scale cirrus fluctuations could hide the sources and the fluctuations of the background they induce. A comparative analysis of the expected power spectra due to (1) cirrus fluctuations in regions of various HI column densities, (2) background fluctuations once sources above the confusion limit have been removed, (3) the detector noise, shows that, in clean regions of the sky ($N_{HI} \leq 1 \times 10^{20}$ atoms cm^{-2}), a survey with 10 mJy *rms* sensitivity should not only detect most sources above the low cirrus fluctuations but could also see background fluctuations in excess of the detector noise fluctuations, on scales 3 to 10 arcmin (see fig.3). Since scenario C has 6.3×10^5 sources/sr with fluxes > 30 mJy, a deep survey of a ~ 1000 arcmin² field

might begin to “break” the CIRB into $\sim 50 \pm 7$ discrete sources, an order of magnitude more than is expected without evolution. This number is sufficient to test the high level of evolution and even begin to disentangle between the various scenarios. If detected, the level of background fluctuations can also help to constrain the redshift distribution of the sources.

The tentative discovery of the Cosmic Infrared Background is now supported by our new study in the cleanest regions of the sky, where the foreground Galactic components are essentially negligible. The conversion of the CIRB into its contributing sources by means of a semi-analytic model of galaxy formation leads to predictions of faint galaxy counts at IR and submm wavelengths. In contrast with the status of IRAS 60 μm counts, 175 μm counts with ISO should be able to detect the predicted strong evolution, and even disentangle between various scenarios consistent with the level of the CIRB. Moreover, small-scale cirrus fluctuations cannot hide the presence of the sources. Consequently, our knowledge of the optical/IR luminosity budget at $z \sim 0.5 - 2.5$ should improve rapidly. We are about to start unveiling the optically-dark side of galaxy formation.

References

- [1] Lilly, S.J., Tresse, L., Hammer, F., Crampton, D. & Le Fèvre, O. The Canada-France Redshift Survey. VI. Evolution of the galaxy luminosity function to $z \sim 1$. *ApJ* **455**, 108-124 (1995).
- [2] Williams, R.E., Blacker, B., Dickinson, M., Van Dyke Dixon, W., Ferguson, H.G., *et al.* The Hubble Deep Field: observations, data reduction, and galaxy photometry. *AJ* **112**, 1335-1389 (1996).
- [3] Lilly, S.J., Le Fèvre, O., Hammer, F., & Crampton, D., The Canada-France Redshift Survey: The luminosity density and star formation history of the universe to $z \sim 1$. *ApJ* **460**, L1-L4 (1996).
- [4] Madau, P., Ferguson, H.C., Dickinson, M.E., Giavalisco, M., Steidel, C.C. & Fruchter, A. High redshift galaxies in the Hubble Deep Field. Color selection and star formation history to $z \sim 4$. *MNRAS* **283**, 1388-1404 (1996).
- [5] Puget, J.L., Abergel, A., Boulanger, F., Bernard, J.P., Burton, W.B., *et al.* Tentative detection of a cosmic far-infrared background with COBE. *A&A* **308**, L5-L8 (1996).
- [6] Soifer, B.T. & Neugebauer, G. The properties of infrared galaxies in the local Universe. *AJ* **101**, 354-361 (1991).

- [7] Hacking, P. & Houck, J.R. A very deep IRAS survey at $l = 97^0$, $b = 30^0$. *ApJSS* **63**, 311-333 (1987).
- [8] Ashby, M.L.N., Hacking, P.B., Houck, J.R., Soifer, B.T. & Weisstein, E.W. A massive $z = 0.088$ supercluster and tests of starburst galaxy evolution at the North Ecliptic Pole. *ApJ* **456**, 428-436 (1996).
- [9] Rowan–Robinson, M., 1997, Mann, R.G., Oliver, S.J., Efstathiou, A., Eaton, N., *et al.*, Observations of the Hubble Deep Field with the Infrared Space Observatory V: Spectral energy distributions, starburst models and star formation history. *MNRAS in press* (1997).
- [10] Reach, W.T., Dwek, E., Fixsen, D.J., Hewagama, T., Mather, J.C., *et al.* Far-infrared spectral observations of the galaxy by COBE. *ApJ* **451**, 188-199 (1995).
- [11] Hartmann, D., & Burton, W.B. *An Atlas of Galactic Neutral Hydrogen Emission*, Cambridge University Press (1995).
- [12] Boulanger, F., Abergel, A., Bernard, J.P., Burton, W.B., Désert, F.X., *et al.* The dust/gas correlation at high Galactic latitude. *A&A* **312**, 256-262 (1996).
- [13] Hauser, M.G. Searching for the Cosmic Infrared Background. in *Unveiling the Cosmic Infrared Background*. E. Dwek, AIP Conference Proceedings 348, 11-21 (1996).
- [14] Lacey, C. & Silk, J. Tidally triggered galaxy formation. I. Evolution of the galaxy luminosity function. *ApJ* **381**, 14-32 (1991).
- [15] Kauffmann, G.A.M., White, S.D.M. & Guiderdoni, B. The formation and evolution of galaxies within merging dark matter haloes. *MNRAS*, **264**, 201-218 (1993).
- [16] Guiderdoni, B., Hivon, E., Bouchet, F.R., Maffei, B., Semi-analytic modelling of galaxy evolution in the IR/submm range. *MNRAS submitted* (1997).
- [17] Hivon, E., Guiderdoni, B., Bouchet, F. *in preparation* (1997).
- [18] Blumenthal, G.R., Faber, S.M., Primack, J.R. & Rees, M.J. Formation of galaxies and large-scale structure with cold dark matter. *Nature* **311**, 517-525 (1984).
- [19] Heyl, J.S., Cole, S., Frenk, C.S. & Navarro, J.F. Galaxy formation in a variety of hierarchical models. *MNRAS* **274**, 755-768 (1995).
- [20] Kennicutt, R.C., Tamblyn, P. & Congdon, C.W. Past and future star formation in disk galaxies. *ApJ* **435**, 22-36 (1994).
- [21] Pascarelle, S.M., Windhorst, R.A., Keel, W.C. & Odewahn, S.C. Sub-galactic clumps at a redshift of 2.39 and implications for galaxy formation. *Nature* **383**, 45-50 (1996).
- [22] Zepf, S.E. & Koo, D.C. Close pairs of galaxies in deep sky surveys. *ApJ* **337**, 34-44 (1989).
- [23] Burkey, J.M., Keel, W.C., Windhorst, R.A. & Franklin, B.E. Galaxy pairs in deep HST images: Evidence for evolution in the galaxy merger rate, *ApJ* **429**, L13-L17 (1994).

- [24] Carlberg, R.G., Pritchett, C.J. & Infante, L. A survey of faint galaxy pairs, *ApJ* **435**, 540-547 (1994).
- [25] Sanders, D.B. & Mirabel, I.F. Luminous infrared galaxies. *ARAA* **34**, 749-792 (1996).
- [26] Soifer, B.T., Sanders, D.B., Madore, B.F., Neugebauer, G., Danielson, G.E., *et al.* The IRAS Bright Galaxy Sample. II. The sample and luminosity function. *ApJ* **320**, 238-257 (1987).
- [27] Lonsdale, C.J., Hacking, P.B., Conrow, T.P. & Rowan–Robinson, M. Galaxy evolution and large-scale structure in the far-infrared. II. The IRAS faint source survey. *ApJ* **358**, 60-80 (1990).
- [28] Rowan–Robinson, M., Saunders, W., Lawrence, A. & Leech, K. The QMW IRAS galaxy catalogue: a highly complete and reliable IRAS 60- μ m galaxy catalogue. *MNRAS* **253**, 485-495 (1991).
- [29] Bertin, E., Dennefeld, M. & Moshir, M. Galaxy evolution at low redshift ? II. Number counts and optical identifications of faint IRAS sources. *A&A* **323**, 685-696 (1997).
- [30] Gautier, T. N., III, Boulanger, F., Perault, M. & Puget, J. L. A calculation of confusion noise due to infrared cirrus. *AJ* **103**, 1313-1324 (1992).

Acknowledgments. We are pleased to thank Dave Clements, François–Xavier Désert, and Bruno Maffei for their comments and suggestions.

Figure Captions

Figure 1: *Inset panel:* High-latitude COBE/FIRAS spectrum in regions with very low HI column densities ($N_{HI} \leq 1 \times 10^{20}$ atoms cm^{-2} , solid line) and residual spectrum after subtraction of emissions correlated with neutral and ionized hydrogen (dotted line). This component is likely to be the Cosmic Infrared Background (CIRB). *Main panel:* The $\pm 1\sigma$ error bars per point have been used to define an acceptable range for CIRB predictions (thick solid lines). Solid squares show the upper limits given by COBE/DIRBE residuals [13]. The solid hexagons show the Cosmic Optical Background obtained by summing up faint galaxy counts down to the Hubble Deep Field limit. Strictly speaking, this is only a lower limit of the actual optical background, but the shallowing of the U and B -band counts suggests near-convergence at least at those wavelengths [2]. The short and long dashes show the background predicted without evolution, in a universe with $H_0 = 50 \text{ km s}^{-1} \text{ Mpc}^{-1}$ and $\Omega_0 = 1$. The solid, dotted and dashed lines show the predictions for our scenarios A, B, and C respectively, in the standard CDM model ($H_0 = 50 \text{ km s}^{-1} \text{ Mpc}^{-1}$, $\Omega_0 = 1$, $\Lambda = 0$, $\Omega_b = 0.05$, and $\sigma_8 = 0.67$). Stars form in cold cores according to Salpeter’s stellar initial mass function (with slope $s = 1.35$, and lower and upper mass cut-offs 0.1 and $120 M_\odot$). Star formation rates are proportional to the cold gas contents, with characteristic time scales derived from the core dynamical times as $t_\star = \beta t_{dyn}$. Scenario A has a mix of two populations, a disk-like one with $\beta = 100$, and starbursts with $\beta = 10$. The mass fraction involved in bursts increases with the formation redshift z_{for} according to $f_{burst} \propto (1 + z_{for})^5$, as suggested by the increasing fraction of pairs seen at larger z [22, 23, 24]. In scenario B and C, we add a population of “ultra-luminous IR galaxies” (ULIRGs) in which all the energy available from stellar nucleosynthesis ($0.007xMc^2$) is radiated by massive stars ($\langle x \rangle = 0.40$) in a heavily-extinguished medium. Scenario B has a 5 % constant mass fraction of ULIRGs at all z_{for} . In scenario C, 90 % of all galaxies forming at $z_{for} \geq 3.5$ are ULIRGs.

Figure 2: Predictions for differential counts normalized to Euclidean counts at $60 \mu\text{m}$

(upper panel) and $200\ \mu\text{m}$ (lower panel). The short and long dashes show the predicted counts without evolution, in a universe with $H_0 = 50\ \text{km s}^{-1}\ \text{Mpc}^{-1}$ and $\Omega_0 = 1$. The solid, dotted and dashed lines show the predictions for our scenarios A, B, and C respectively in the SCDM model (see text). Data are plotted for IRAS counts at $60\ \mu\text{m}$. Open stars: Faint Source Survey [27]. Open squares: QMW survey [28]. Solid squares: North Ecliptic Pole Region [7]. The IRAS $60\ \mu\text{m}$ counts suggest some evolution, but do not discriminate between the various scenarios. These scenarios also predict a $60\ \mu\text{m}$ background fluctuation per beam in the Very Faint Source Survey (after removal of $\geq 4\sigma_{tot} = 120\ \text{mJy}$ sources) at the level of $14.1\ \text{mJy}$ (A), $16.0\ \text{mJy}$ (B), and $14.3\ \text{mJy}$ (C), while the measured 68 % quantile is $30.1 \pm 1.2\ \text{mJy}$ [29]. With a $25\ \text{mJy}$ *rms* instrumental noise and $6.5\ \text{mJy}$ *rms* cirrus fluctuations [30], there is still space for a $15.4^{+2.2}_{-2.5}\ \text{mJy}$ fluctuation due to sources, in good agreement with our estimates. In contrast, scenarios A, B, C predict much stronger evolution at $200\ \mu\text{m}$. The differences in the predicted counts originate from the differences in the high-redshift IR emissions.

Figure 3: Comparison of predicted power spectra for observations in the ISO C160 filter. The straight horizontal lines (same code as in fig.1) show the predicted background fluctuations at the confusion limit (i.e. its *rms* value equals one third of the limiting flux of all resolved and removed sources). The beam was modelled as a 1 arcmin FWHM gaussian. The cirrus fluctuations (thin lines) are described by a k^{-3} power law [30] with levels (from left to right) set by column densities of neutral hydrogen (HI) respectively typical of the Lockman hole (minimum, 0.24 % of the sky), and of 4.6 %, & 21.8 % of the sky. The detector noise spectrum of fluctuations (thin dashed lines), assumed to be white, is shown for a sensitivity level of 10 and 20 mJy per 1.5 arcmin pixel. To allow for a direct comparison, this flat white noise has been projected on the sky, i.e. divided by the Fourier transform of the beam profile. The resulting exponential rise of the on-sky noise thus bounds the range of available scales. The comparison shows that, in the cleanest regions of the sky, (e.g. $N_{HI} = 1 \times 10^{20}$

atoms cm^{-2}), unresolved background fluctuations for scenarios B and C actually dominate both cirrus and noise fluctuations at scales $3 < \theta < 10$ arcmin, if the *rms* noise level is 10 mJy per pixel.

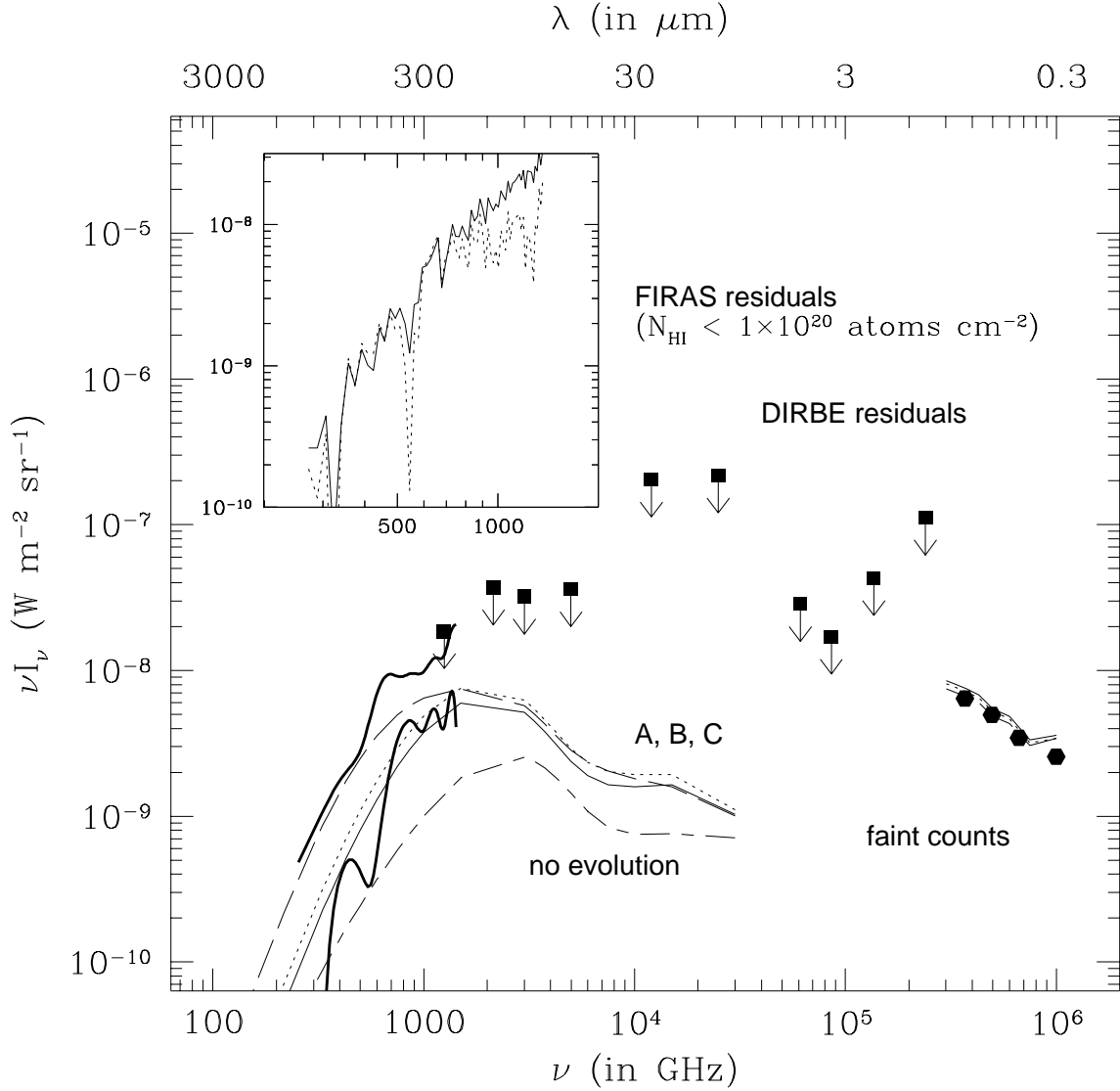


Figure 1:

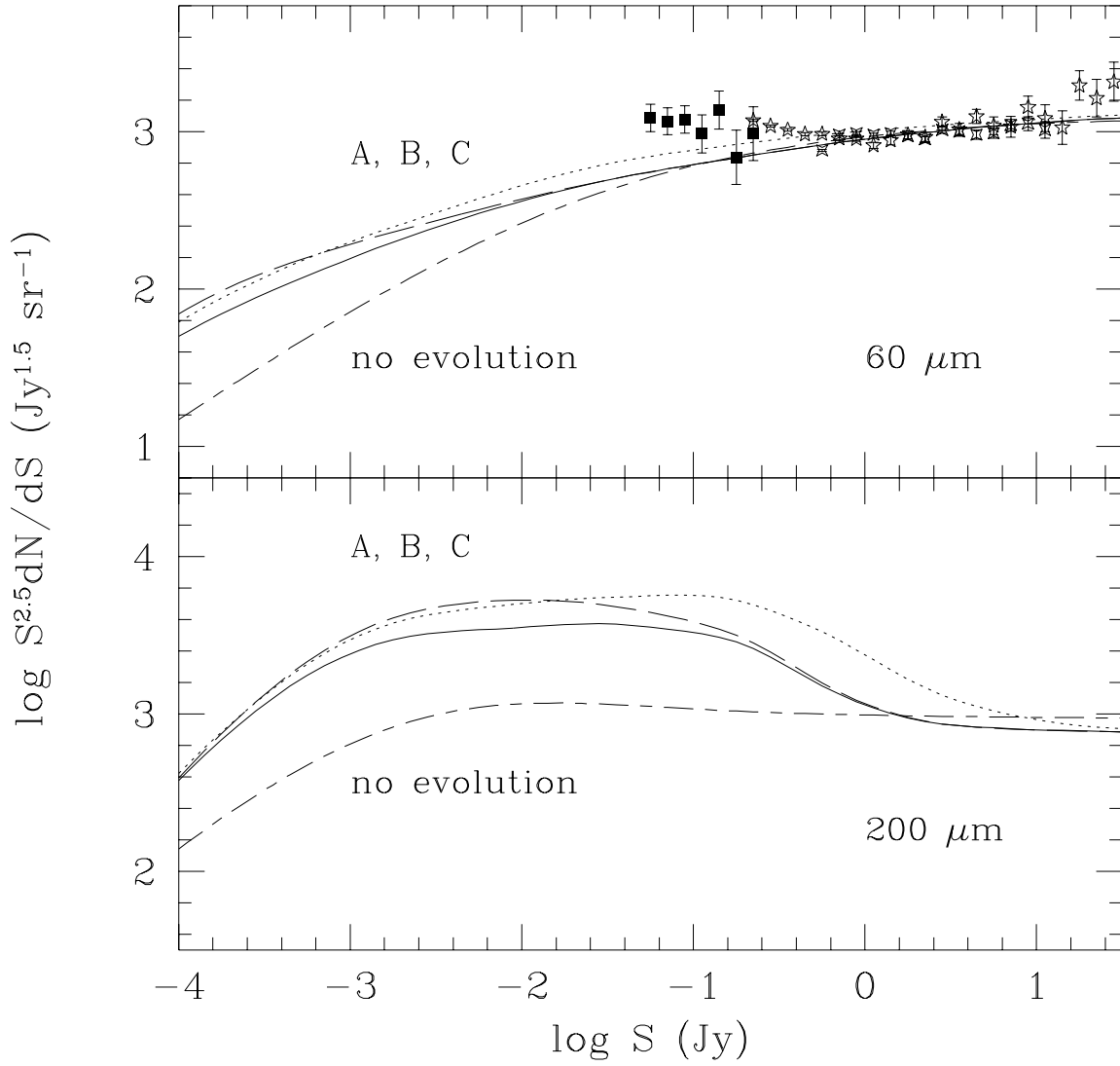


Figure 2:

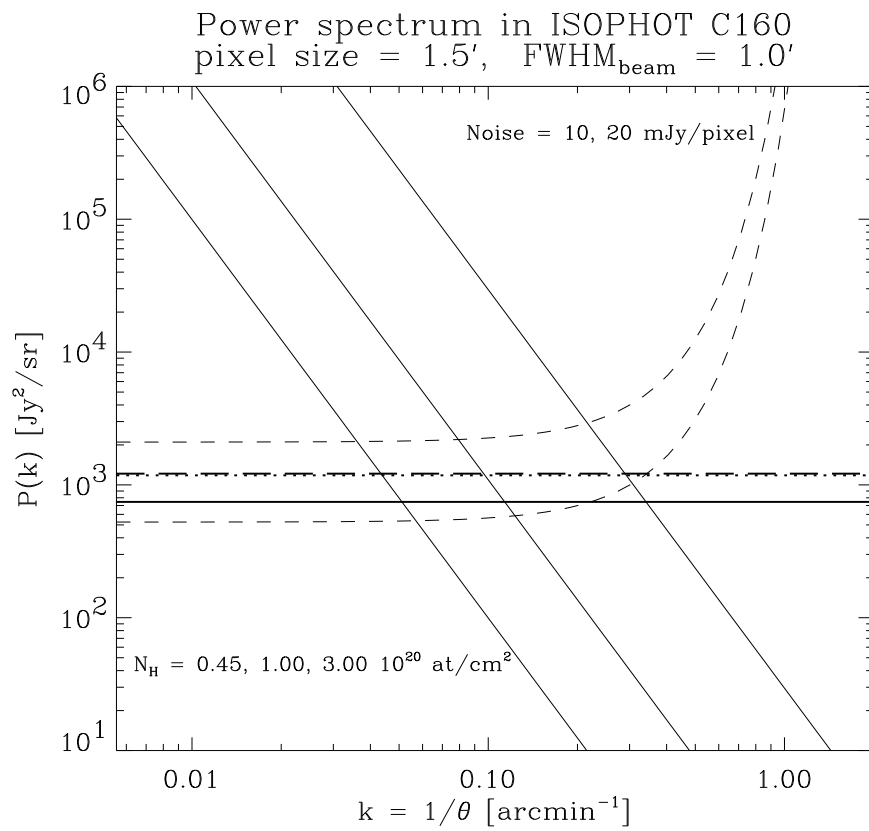


Figure 3: